

SFSA Cast In Steel 2026 – Horseman's Axe

Technical Report

Mississippi State University – Headless Dawgmen



CENTER FOR ADVANCED
VEHICULAR SYSTEMS



Team Members:

Bryant Applegarth, Andrew Eakes, Hayley Gilmer, Wilton-Mark Pettus, William Raber

Advisor(s) Name:

Blake Stewart (Primary) and Tim Shaw (Secondary)

Foundry Partner:

Southern Cast Products, Meridian, Mississippi

Introduction

The Steel Founders' Society of America (SFSA) Cast in Steel (CIS) competition is an annual event that challenges students from universities across the country to design and manufacture steel weapons and tools using modern casting techniques. SFSA has created this competition to encourage students to learn about making steel products using the casting process and applying the latest technology available. For the 2026 CIS competition, teams have been tasked with producing a horseman's axe by casting while remaining historically authentic. This report details the research, design, production, and testing behind Mississippi State University's (MSU) submission for CIS 2026.

Historical Background

The horseman's axe is one of the most distinctive and specialized weapons ever developed for mounted combat. In general, these axes are characterized as a battle-axe used by cavalry. Most accounts described the horseman's axe as being small enough to be wielded with one hand and having features that include a curved blade, a spike on the top, and a spike on the side opposite the axe blade (known as a pick). To contextualize the horseman's axe, a historical deep dive of key technological advancements and weapons development is necessary.

Dating to the Stone Age (~ 3.3 million BC - 4000 BC), axes were simple hand tools with stones chipped to a point that were used for a variety of tasks including butchering and digging as shown in Figure 1. Over time, wooden handles were introduced to improve leverage where they were initially secured using leather or rope bindings. Later refinements, further shown in Figure 1, incorporated holes in the axe head, allowing for the head to be attached more securely (Ref 1).

The Bronze Age (~ 3300 BC – 1200 BC) introduced many innovations that influenced the evolution of axes used in mounted combat including the domestication of the horse and advancements in axe design. According to the Smithsonian, horse domestication was believed to originate in the Pontic-Steppe, a grassland region in Eastern Europe and Western Asia extending from north of the Black Sea to the Caspian Sea, around 2200 BC (Ref 2). The domestication of the horse allowed for the possibility of mounted combat. Furthermore, the Bronze Age saw several innovations in axe design, including socketed and palstave axe heads seen in Figure 2 (Ref 3). These developments enhanced their effectiveness as both tools and weapons. However, limitations of materials (copper and bronze) and manufacturing methods (early adaptations of casting) available during the time kept the axes smaller and less specialized compared with axes from later time periods (Ref 4).

The Iron Age (~ 1200 BC – 550 BC) built on the innovations of the Bronze Age, further refining axe designs with shapes and forms increasingly resembling modern axe designs as well as utilizing advancements in horse domestication. In particular, the introduction of iron as a material allowed axes to become larger and broader compared to the axes of the Bronze Age (Ref 1). It was also around this period where mounted combat became increasingly prominent where it would evolve out of the Pontic-Steppe region around 1000 BC. From the Pontic-Steppe region, Turchin et al. noted the spread of mounted combat to nearby regions in Europe, Africa, and Asia which is highlighted in Figure 3 (Ref 5). This widespread adoption was likely attributed to the invention of equestrian equipment such as bridles and harnesses that improved handling and control during the Bronze Age. These improvements allowed combatants to use weapons more effectively while riding on horseback (Ref 6). The Scythians, a nomadic tribe that roamed Central Asia from 900 BC to 200 BC, were among the earliest groups to effectively employ weapons on horseback (Ref 7). The Greeks, when they first encountered the Scythians, noted their effectiveness by illustrating them as the mythological icon known as the Centaur (Ref 8). While the Scythians' weapon of choice was the bow and arrow, they were also one of the earliest civilizations to use battle-axes fitting the general description of a horseman's axe, a battle-axe mixed with a pickaxe. Known

as the Sagaris, this weapon was said to puncture the skulls of combatants and humanely end the lives of their horses when required; however, there is limited evidence to suggest that it was specifically used as a mounted weapon in the same context as what the horseman's axe was known to be within Medieval times. Figure 4 shows a depiction of the Sagaris found on Greek pottery (Ref 10). In the depiction, the shape of the axe head is like the more well-known horseman's axes of the 14th to 17th centuries, but the axe head is much smaller, and a spike is not present.

The Medieval Age (~ AD 500 – AD 1500) brought more specialized axes across various regions of Europe. In particular, Vikings within the Scandinavian region created the bearded axe and Dane axe shown in Figure 5 and Figure 6, respectively, that incorporated foundational design features by combining curved blades, extended cutting surfaces, and improved weapon balance which likely heavily influenced the horseman's axe design seen later in the Medieval period (Ref 11,12). By the time of the Battle of Hastings (AD 1066), battle-axes were well established as a primary weapon of choice by ground soldiers, as depicted in the Bayeux Tapestry in Figure 7. While the Bayeux Tapestry does not show any combatants wielding an axe on horseback, many combatants are seen countering cavalry with battle-axes, showing its capability to fight back against mounted troops (Ref 13). Beyond this, the popularity of battle-axes among nobility is also noted from the Battle of Lincoln (AD 1141). Contemporary accounts describe King Stephen of England becoming surrounded by opposing forces and initially defending himself with a sword. However, during the fighting, his sword broke and a nearby soldier handed him a battle-axe to continue fighting (Ref 14).

One of the earliest notable instances aligning with modern interpretations of the horseman's axe is found from the historical account of the Battle of Bannockburn (AD 1314). During the battle, Robert the Bruce rode towards Henry de Bohun on horseback with an axe in hand. In their confrontation, Robert the Bruce embedded his axe into the head of Henry de Bohun, brutally defeating him. From historical accounts, Henry's helmet was made of steel plate armor, suggesting that the axe used by Robert the Bruce was powerful enough to penetrate heavy armor and deliver a deadly blow. A depiction of this battle is shown in the *Holkham Bible Picture Book* (AD 1330), where Figure 8 highlights Robert and Henry's bout (Ref 15). In the depiction, an axe with the general features of the modern horseman's axe is visible, including the axe blade, top spike, and pick combination.

Horseman's axes within museum collections first date back to the 15th century. One of the earliest examples found of the horseman's axe in museum collections dates back to AD 1475 where the weapon features the typical blade, spike, and pick combination (Ref 16). This battle-axe, shown in Figure 9, features a crescent-shaped appearance, likely to take advantage of the momentum of the horse along with the angle and path of where the axe could swing. The elongated spike on top appears suitable for thrusting actions while a slightly angled design of the pick allows for more force concentration in the downward motion of the pick. The axe head appears to be a separate piece from the spike and handle where it is mechanically secured to the handle with a pin. This axe also incorporates long metal strips on the sides of the axe, otherwise known as langets, that would protect the handle from damage during battle and provide strength (Ref 17). Furthermore, a belt loop is seen attached to one side, likely allowing the wielder to secure the weapon while riding. Finally, small holes can be seen towards the bottom that suggest the use of a wrist strap that was likely used to reduced risks of losing the axe when swinging in battle.

Additional examples of horseman's axes can be seen in Figure 10. The axe shown on the left is a more ornamental axe, evidenced by the faded gilt (gold-colored decoration) on the axe and intricate engravings on the axe head, while the axe on the right is more suited for combat. The ornamental axe still retains the prominent features of a horseman's axe with the crescent shaped blade, elongated top spike, pick, and langets on the side (Ref 18). More interestingly is that this axe appears to contain all three features on a

single, continuous piece as opposed to the spike being a separate piece as seen in other designs. The battle-axe again shows a crescent shape but with more angular transitions on the upper and lower edges, giving it a sharper profile compared to the ornamental axe. This axe features brass langets to reinforce the sides, and the axe head is attached with a pin to the handle (Ref 19). Some variations of horseman's axes did not feature the addition of langets, as seen in Figure 11 (Ref 20,21). The axe on the left features a unique design where the entire handle is made of metal and includes a disc guard. The axe on the right also does not contain any langets and has a handle made of wood. This axe does not feature a spike, indicating that not every horseman's axe used a spike, and includes a wrist strap made of thin rope that is loose enough likely to allow the wielder to quickly slip their hand in during combat. Of these horseman's axes, none of them weighed more than 3 lbs or had a length over 3 ft with details provided in Table 1. These limitations were likely made to keep the weapon wieldable while maneuvering the horse.

From evidence predating AD 1400, support for the horseman's axe was traced through historical discussions, artistic depictions, and archaeological findings which all lead to the development of the axes that are preserved in 14th – 17th century museum collections. These historical findings were therefore heavily considered and incorporated into the axe design for this competition.

Axe Design

The design process began with the previously discussed research into historical axes. The features and dimensions of these axes were carefully studied to ensure historical accuracy was preserved. Many of these axes share commonality in having a pick, spike, and blade and a handle of one of various styles, which include wood and steel. Robert the Bruce's weapon is what is most often referred to for horseman's axes, so it was determined that the axe design should closely resemble the style of that period (early 14th century). These axes often had wood handles with metal langets to protect the handle and improve strength. Typical historical designs involved the langets being formed with the spike while the blade and pick were a separate piece. These would then be inserted together and pinned to the handle (Ref 17).

Based on the historical context and examples analyzed, many features were included in the axe design for this competition. The axe blade was designed to have a crescent-like shape to account for the various swinging angles from horseback. An elongated spike was also included due to its frequent presence in historical designs, suggesting it played an integral role in the weapon's functionality and effectiveness in mounted combat. The spike was likely used for thrusting and was therefore designed to be approximately 3" long to be able to penetrate vital organs. A pick with a slight downward taper was selected as this shape would concentrate force to deal significant damage to plate armor. Accessories included that are seen on historical horseman's axes are a leather wrist strap to allow better retention of the weapon and a belt loop near the top for sheathing the weapon while riding.

In order to strike a balance between maintaining structural integrity, observing historical precedence, and applying an innovative casting design, the basis of the axe design was such that MSU's industry partner, Southern Cast Products (Meridian, MS), would cast the head (blade, pick, and spike) as a single piece while the langets would be cast and rolled in the Center for Advanced Vehicular Systems' (CAVS) in-house facilities, later connecting them with brass pins. SolidWorks was utilized to create a 3D model of the axe with a comparison between the initial and final designs being shown in Figure 12. In collaboration with Southern Cast Products, dimensions and details of the axe were adjusted to ensure molten metal could fill all features of the part while minimizing porosity. These changes included a larger radius of the axe head, a tapered blade, and a simplified geometry of the pick. Following these changes, a "handle" was modeled to represent the added weight of two 0.125"x0.5"x24" steel langets, a 28" wood handle, and the brass pins. SolidWorks then provided an estimated mass of the completed axe. Various dimensional changes and chamfers were added to decrease the estimated mass within a safe margin error to ensure

the maximum weight was not exceeded. To cast the head, the gating system would include a single runner attached to the bottom face of the axe where the handle insertion would later be machined. This was fed from a large sprue that also functioned as a riser during solidification.

The steel alloy used for casting was based on current production schedule at Southern Cast Products. In previous Cast in Steel competitions, MSU used a mining tooth alloy (CS1E0703) that was frequently cast at Southern Cast Products. Although the initial plan was to use this alloy again given its performance in previous SFSA competitions (2019 and 2020), one of which was a different style of axe, this alloy was not available in the production schedule within allotted time for this competition. Therefore, another alloy, CS-28A, was determined to be the best fit from hardness and strength simulations performed with JMatPro-v151. The target compositions of both alloys and the measured axe alloy composition can be seen in Table 2. Utilizing the Jominy end quench simulations for both alloys, the CS-28A alloy provides a similar hardness value of ~50 HRC and a tensile stress of roughly 1900 MPa (as quenched) in comparison to ~52.5 HRC and 2000 MPa for CS1E0703 as seen in Figure 13. Comparing continuous cooling transformation (CCT) diagrams for both materials, shown in Figure 14, it was seen that there was a slight rightward shift of the ferrite and pearlite curves and a leftward shift of the bainite curves. The rightward shift indicated that it would be easier to obtain the harder phases (bainite and martensite). However, the leftward shift of the bainite curves indicated a more rapid cooling rate would be necessary to obtain pure martensite.

The most common wood species historically used for axe handles were maple, hickory, and ash. Each was a viable option for a handle, but ash was ultimately selected through elimination. Hickory was not available in Europe during that time period, eliminating it as an option. Between ash and maple, ash was selected because it had a lower stiffness than maple, allowing for more shock absorption from an impact against a hard object (e.g. armor, shield etc.). Historical axes in Europe would have likely used European ash, *Fraxinus Excelsior*, but white ash, *Fraxinus Americana*, was selected instead because no distributor could be identified to obtain European ash within a reasonable timeframe for this competition (Ref 17,22). To ensure long-term preservation of the axe handle, a sealant was desirable to be applied to the handle to prevent degradation or rotting due to moisture exposure. In the pursuit of historical accuracy, linseed oil was used as it has been used since ancient times with the oldest known use being in ancient Egypt with the linen rags of King Tut's (died 1334 BC) mummy (Ref 23). Linseed oil was also used as a finish on furniture in the Medieval Period (11th to 16th Centuries) (Ref 24). There are scarce historical records of the use of linseed oil on tool and weapon handles, but since it was used on wood at the time and is used on wooden handles today, it can be intuited that the handle of a horseman's axe could have been finished with linseed oil. Natural linseed oil dries very slowly; therefore, boiled linseed oil was selected due to its faster drying time (Ref 25,26). To preserve the axe head, rust inhibitor (CR 3-36) was selected. Overall, the design features chosen utilized modern techniques while maintaining historical authenticity.

Casting and Construction Methodology

Sand mold casting was used as the casting process since it is the specialization of Southern Cast Products. The molds were constructed by MSU while the casting was performed by Southern Cast Products. ABS plastic was used to print two halves of the 3D model of the axe head to serve as the patterns. The mold boxes were approximately 12"x12" at the intersection of the cope and drag with the walls featuring 5° draft angles. The interior surfaces of the molds were sanded to ensure an easy mold release with large voids being filled with epoxy. The patterns were also sanded and fixed to the molds with dowel rods to ensure alignment. The completed molds are shown in Figure 15.

Southern Cast Products designed the risers, sprues, and gates for the molds using their casting software and installed them into the mold boxes. Six axe heads were subsequently cast, as shown in Figure 16. Prior

to removing the risers, the axe heads were annealed at 950°C for 1 hour before being furnace cooled (Ref 27). This was done to soften the steel and relieve internal stress to ease further processing. After riser removal, each axe head was inspected and compared to ensure the best head was selected, minimizing deep surface pores, incomplete features, and other defects.

Belt grinding was used to perform the shaping and finishing of the axe head to remove any surface defects as well as to machine the primary bevel leading to the sharpened edge (secondary bevel). For modern axes, primary bevel angles range from 20 to 40 degrees with the secondary bevel being 5 degrees greater than the primary (Ref 28). To balance sharpness and durability, a 30-degree primary bevel and a 35-degree secondary bevel were used. The hole (also known as the eye) for the handle was designed in SolidWorks to ensure that the head would remain sufficiently thick around the handle. The best-fit shape was determined to be a 1.5" × 0.75" oval at 0.68" depth. This was done using a manual mill with a 0.75" flat end mill as shown in Figure 17.

After all machining and grinding were completed, the final heat treatment was applied to the axe. A microstructure of tempered martensite was selected due to the high hardness obtained with martensite and the increased ductility and toughness with the tempering process (Ref 29). The axe was heated to a temperature of 850°C for 1 hour (see Nondestructive Testing and Analysis) and then saltwater quenched to provide the cooling rate required to obtain a fully martensitic structure. Tempering was performed at 200°C for 1 hour (see Nondestructive Testing and Analysis). After quenching and tempering, final grinding and polishing of the axe head were completed to obtain fine details and the desired surface finishes. The pin holes for the langets in the axe head were drilled after the heat treatment to prevent scale from forming inside the holes. The axe head was then finished by sanding up to 400 grit sandpaper.

The as-received white ash used for the handle was approximately 2"x2"x24", as shown in Figure 18. This blank was planed and sanded to obtain a cross-section of approximately 1"x1.5". The mating end of the handle was formed by sanding 0.73" of the length to a profile that fit snugly within the eye. This end was then shortened until it contoured the bottom of the axe head. To ensure the langets maintained consistent contact across the handle and axe head, the handle was sanded to be flush to the sides of the axe head. The handle was then rounded into a flattened oval of 0.95"x1.5". The bottom of the handle, where a user would grasp the axe, was tapered into a slight hourglass shape to improve the grip. The handle at this stage is shown in Figure 19. Three coats of boiled linseed oil were then applied for the final finish.

The langets and belt loop were produced from a steel casting at CAVS's facility. The ingot was hot rolled to a thickness of 0.24" as seen in Figure 20, pickled to remove scale, and cold rolled to a final thickness of 0.08", as seen in Figure 21 and Figure 22. The langets and belt loop were then cut from the plate using a water jet with specified dimensions of 0.5"x24" and 0.5"x6", as seen in Figure 23 and Figure 24. Four 0.25" holes were drilled through each of the langets starting 0.5" from the bottom and spaced 3.5" apart, center-to-center, along the length. The langets were then clamped along the center of the handle, and the langet holes were used as guides for drilling pinholes into the handle. The top of the langets were trimmed to length, forged, and ground to match the profile of the axe head. The langets were finally annealed at 500°C for 1 hour and cooled to room temperature to restore the steel's ductility after cold rolling (Ref 30). The belt loop was forged by hand to the shape seen in Figure 25. The pinhole was drilled in the loop for mounting to the axe head, and the excess was removed ensuring the profile matched with the langets and axe head. The langets were polished with sandpaper up to 2000 grit and buffed with Green Rogue (chromium oxide) polishing compound to obtain their final finish while the belt loop was sanded to a 400 grit finish. The final langets and belt loop can be seen in Figure 26.

Lastly, the components were assembled. The brass pins were forged into the pinholes, forcing them to expand, in conjunction with epoxy, to attach the head, langets, and belt loop to the assembly. The axe head was finally sharpened and coated with CR 3-36, producing the final product.

Nondestructive Testing and Analysis

The axe head and riser material from the casting were used to perform non-destructive testing and analyses to characterize the properties of the axe. The non-destructive tests that were performed included X-Ray computed tomography (CT), optical microscopy, and Vickers microhardness testing. Analytical testing included the creation of continuous cooling transformation (CCT) diagrams, Jominy end quench, flow stress, and tempering simulations using JMatPro-v151, and finite element analysis (FEA) using 3DS Simulia Abaqus.

X-Ray CT scans were performed after annealing and scale removal to help identify any pores within the axe head. Large pores could create areas of high stress concentration, potentially leading to cracking when the axe head is impacted. A large pore present in the spike, for example, may cause the end of the spike to break off when it is thrust into an object. The blade, spike, and pick are shown in Figure 27, Figure 28, and Figure 29, respectively. The most significant pores identified within the axe head are around the cheeks and spike. No measurements were taken of the pores at the time of measurement, but based on the scale of the part, the pores are approximately 1mm in diameter. Most of these pores were very close to the edges of the axe and were removed during grinding.

After annealing, 3 specimens were cut from the riser material. These specimens were subjected to heat treatments which characterized each stage in the axe head's conclusive heat treatment. The specimens were polished up to a 0.02 μm polishing solution and etched with 2% nital. Micrographs were taken and analyzed to characterize the microstructure at each point of the heat treatment process. The quenched specimens were additionally etched with 10% sodium metabisulfite (SMB), and additional micrographs were taken. The micrographs are provided in Figure 30, Figure 37, and Figure 38 for the annealed, quenched, and quenched and tempered cases, respectively.

The first specimen was annealed and was used in accordance with ASTM Standard EM112-25, providing an average grain size of $24.68 \pm 2.02 \mu\text{m}$ ($n=4$) (Ref 31). JMatPro-v151 was utilized to create various simulations for the alloy used for the axe. The CCT diagrams showed an austenization temperature of 828 $^{\circ}\text{C}$, 50 $^{\circ}\text{C}$ above A_3 , as seen in Figure 31. To ensure a fully austenitic structure, the temperature for the austenization process of the axe was increased to 850 $^{\circ}\text{C}$. The as-quenched yield strength and hardness were estimated by Jominy hardenability simulations to be $\sim 1625 \text{ MPa}$ and $\sim 50 \text{ HRC}$, respectively, as seen in Figure 32. Tempering simulations, as seen in Figure 33, showed that 200 $^{\circ}\text{C}$ produced the best fracture toughness. The hold time was also simulated as seen in Figure 34, Figure 35, and Figure 36. Since there was minimal change over two hours, one hour was selected to ensure that the toughness values were acceptable.

The next two specimens followed the quench and quench and tempering processes as determined by JMatPro-v151. One specimen would be austenitized at 850 $^{\circ}\text{C}$ for 1 hour and quenched while the other would additionally be tempered at 200 $^{\circ}\text{C}$ for 1 hour. The micrographs for the quenched and quenched and tempered specimens are shown in Figure 37 and Figure 38, respectively. Figure 38 shows a tempered martensitic structure, as was desired. The quenched sample showed a Vickers microhardness value of $510 \pm 10 \text{ HV}$ ($n=50$) with the values plotted in Figure 39. The quenched and tempered sample, in comparison, obtained a Vickers microhardness value of $501 \pm 22 \text{ HV}$ ($n=800$) with the values similarly shown in Figure 40. Southern Cast Products provided various mechanical testing results of the as-cast material, as shown in Table 3. Using a conversion table (Ref 32), the quenched and tempered specimen had a Vickers hardness value that corresponds to a hardness value of 51 HRC. Compared to the hardness value of the as-cast

material, which was 37 HRC at its maximum, this shows a significant improvement in strength. The hardness of the tempered specimen was used for a flow stress simulation to produce an estimated tensile stress of 1655 MPa, as seen in Figure 41. This tensile strength was higher than the strength that tempering was predicted to produce, which was 1493 MPa as previously seen in Figure 36, 10.9 % higher than the initial prediction.

FEA was conducted using 3DS Simulia Abaqus to evaluate the structural response of the axe under realistic loading conditions expected during horseback combat. The horseman's axe model used for this simulation can be viewed in Figure 42. Table 4 displays the general setup of the FEA simulation where true stress and true strain in the plastic assumption were calculated using Equation 1 and Equation 2. Figure 43, Figure 44, and Figure 45 illustrate the various pressures applied to simulate realistic combat uses of the horseman's axe. The handle was treated as a static, rigid body where the axe head was allowed to deform under applied loads. The force applied in the simulation was calculated using Equation 3, Equation 4, and Equation 5. This force was then scaled according to the areas over which the pressures were applied. Estimations such as an average horse height of 2 meters along with an impact duration of 0.5 ms for steel-on-steel contact were considered in these calculations (Ref 33). The mesh of the axe head can be seen in Figure 46. Figure 47, Figure 48, and Figure 49 show the resulting von Mises stress contours from each of the simulations. From the loading conditions applied, the weapon is expected to perform well under the tests that it may be subjected to in the competition. Striking closer to the center shows a better structural response while striking near the lower edge shows more stress concentration signifying the axe can handle combat-level strikes. High stress concentrations in the pick indicate that it delivers substantial localized impact to the plate metal.

Final Results

MSU's submission for Cast in Steel 2026 is a horseman's axe that blends both historical precedent and modern practices for its design. The finished weapon is shown in Figure 50. The total length of the axe was 27.5", and the weight was 1.95 lbs, which were well within the size limits of 31.5" and 3.3 lbs as seen in Figure 51 and Figure 52. Other measurements include the length of the blade (4.3125"), spike (3"), and pick (2.5"). The center of balance was 9" from the tip of the spike. The compactness of the head lowered the overall weight and improved its handling while remaining deadly. Its lethality was enhanced by the langets, whose structural support allows the axe to be swung with greater force while protecting the handle from opponents. The properties of the axe were also evaluated through nondestructive testing and analyses to ensure that the axe would have the desired quality. A ballistic gel head and torso dummy from Ballistic Dummy Lab was obtained for real world validation as seen in Figure 53. The engineering design of the weapon is brought out further by its aesthetic design, which is not only pleasing to the eye but period accurate. Based on the features, methodologies, and research described in the report, this axe will stand out among competitors.

References

1. Gransfors Bruk Sweden, "History of the Axe," *Gransfors Bruk*, n.d. <https://www.gransforsbruk.com/en/the-axe-guide/history-of-the-axe>. Accessed 18 March 2026
2. Christian Thorsberg, "When Did Humans Domesticate Horses? Scientists Find Modern Lineage Has Origins 4,200 Years Ago," *Smithsonian magazine*, 2024. <https://www.smithsonianmag.com/smart-news/when-did-humans-domesticate-horses-scientists-find-modern-lineage-has-origins-4200-years-ago-180984483/>
3. Timothy Bromm, "The Axe and Man," *Bromm*, 2014. <https://timothybromm.wordpress.com/2014/10/06/the-axe-and-man/>
4. Florin Curta, Copper and Bronze: The Far-Reaching Consequences of Metallurgy, *Impact of Materials on Society*, 2022. https://eng.libretexts.org/Under_Construction/Impact_of_Materials_on_Society/05%3A_Copper_and_Bronze_The_Far-Reaching_Consequences_of_Metallurgy
5. P. Turchin, T.E. Currie, and E.A.L. Turner, Mapping the Spread of Mounted Warfare, *CDN*, 2017, **7**(2). <https://doi.org/10.21237/C7CLIO7233509>
6. Noor Haider, "The History of Horse Bits: From Ancient Bone to Modern Stainless Steel," *Cavalon*, 2025. <https://cavalonbits.com/blogs/information/the-history-of-horse-bits-from-ancient-bone-to-modern-stainless-steel>
7. John Stanley, "Archery History: Horseback Archers of the East, Orient and Ancient World," *World Archery*, 2020. <https://www.worldarchery.sport/news/178461/archery-history-horseback-archers-east-orient-and-ancient-world-1>
8. Harvey Nash, The Centaur's Origin: A Psychological Perspective, *The Classical World*, 1984, **77**(5), p 19. <https://doi.org/10.2307/4349592>
9. British Museum, "Introducing the Scythians," *Introducing the Scythians*, 2017. <https://www.britishmuseum.org/blog/introducing-scythians>. Accessed 18 March 2026
10. manière d' Euphronios, "Amphore G106," 510. <https://collections.louvre.fr/ark:/53355/cl010269997>. Accessed 18 March 2026
11. Norsegrade, "The Legacy of Viking Axes: Tools, Weapons, and Symbols of Power," *Norsegrade*, n.d. https://www.norsegarde.com/blogs/lore-and-mythology/the-legacy-of-viking-axes?srsItd=AfmBOopolh15WljrgrAYCipc_9-oOd3Jd8BF_auZXqNNiHrJGmJeqazV
12. Rolf Fabricius Warming, "Artefact of the Month: The Dane Axe," *Society for Combat Archaeology*, 2014. <https://combatarchaeology.org/artefact-of-the-month-the-dane-axe/>
13. Bayeux Museum, "Discover the Bayeux Tapestry," *Bayeux Museum*, Bayeux Museum, n.d. <https://www.bayeuxmuseum.com/en/the-bayeux-tapestry/discover-the-bayeux-tapestry/>
14. Sharon Bennett Connolly, "The First Battle of Lincoln, 1141," *Hisotry...The Interesting Bits!*, 2020. <https://historytheinterestingbits.com/2020/07/18/the-first-battle-of-lincoln-1141/>
15. T.W. Coke, "Holkham Bible Picture Book," (British Library Archives and Manuscripts Catalogue), British Library, 1327. <https://searcharchives.bl.uk/catalog/040-002104030>. Accessed 18 March 2026
16. William McPeak, "The Battle-Ax," *Warefare History Network*, Sovereign Media, 2011. <https://warfarehistorynetwork.com/article/the-battle-ax/>
17. Craig Johnson, "What Are Langets on a Polearm For?," *Arms & Armor*, 2020. <https://www.arms-n-armor.com/blogs/news/what-are-langets-on-a-polearm-for>. Accessed 18 March 2026
18. Cardinal Ippolito de' Medici, "Horseman's Ax of Cardinal Ippolito de' Medici," 1530. <https://www.metmuseum.org/art/collection/search/26548>. Accessed 18 March 2026
19. George F. Harding Collection, "Horseman's Axe," 1490. <https://www.artic.edu/artworks/116956/horseman-s-axe>. Accessed 18 March 2026

20. "Axe - VIII.98," 1600. <https://royalarmouries.org/collection/object/object-1472>. Accessed 18 March 2026
21. The John Woodman Higgins Armory Collection, "Horseman's Axe," Head 1500s; Haft 1800s. <https://worcester.emuseum.com/objects/48760/horsemans-axe>. Accessed 18 March 2026
22. Jeremy aka The AXEMAN, "Selecting the Right Wood for Your Axe Handle," 2024. <https://axeman.ca/blogs/news/selecting-the-right-wood-for-your-axe-handle>. Accessed 18 March 2026
23. Livius, "King Tut's Mummy Slow-Cooked by Its Own Wrapping," *The History Blog*, 2013. <https://www.thehistoryblog.com/archives/27770>
24. Stanley D. Hunter, "Medieval Furniture," 2001. https://visualelbolson.wordpress.com/wp-content/uploads/2015/04/furniture_class.pdf
25. Jim Bell, "How to Oil Finish an Axe Handle (for the Best Results) | Axe & Tool," *Axe&Tool*, 2026. <https://axeandtool.com/oil-your-axe-handle/>. Accessed 18 March 2026
26. Ardec, "Linseed Oil, a Natural Solution for Wood Finishing," *Ardec - Finishing Products*, 2015. <https://artdec.ca/en/blog/22/linseed-oil-a-natural-solution-for-wood-finishing>. Accessed 18 March 2026
27. Gateway Metals Inc., "A Simplified Guide to Heat Treating Tool Steels," *Gateway Metals Inc.*, n.d. <https://gatewaymetals.com/a-simplified-guide-to-heat-treating-tool-steels/#:~:text=Austenitizing%20depends%20upon%20time%20and,of%20furnace%20time%2C%20never%20soaked>.
28. Rich Colvin, "Axes & Hand Axes," *Sharpening Handbook*, n.d. <https://www.sharpeninghandbook.info/GT-Axe.html>. Accessed 18 March 2026
29. Christopher Cahill, Bryan Jung, Omesh Kamat, and Miles Schuler, "EVOLUTION OF MATERIALS IN ARMS AND ARMORS: MEDIEVAL ERA BATTLE AXE," 2015. <https://web.wpi.edu/academics/me/IMDC/IQP%20Website/reports/1415/medieval.pdf>
30. Metal Zenith, "Recrystallization Temperature: Key to Steel Microstructure Control," *Heat Treatment & Processing Terms*, 2025. https://metalzenith.com/blogs/heat-treatment-processing-terms/recrystallization-temperature-key-to-steel-microstructure-control#google_vignette
31. "Standard Test Methods for Determining Average Grain Size," (West Conshohocken, PA), 2025. store.astm.org/e0112-25.html. Accessed 18 March 2026
32. OnlineMetals, "Hardness To Tensile Conversion Table," *OnlineMetals*, n.d. https://www.onlinemetals.com/en/hardness-conversion-table?srsId=AfmBOorgkFqu3IPoNYJm1XWDsP-Bf2a4nvSw_p6QOWjmXINSsBN8_kCf
33. N.B. Muhammad Said, M.B. Ali, K.A. Zakaria, and M.A.M. Daud, Comparison of Impact Duration Between Experiment and Theory From Charpy Impact Test, *MATEC Web Conf.*, S. Sharif, M.M.A.B. Abdullah, S.Z. Abd Rahim, M.F. Ghazali, N. Mat Saad, M.M. Ramli, S.A. Zainol Murad, and S.S. Mat Isa, Eds., 2016, **78**, p 01054. <https://doi.org/10.1051/matecconf/20167801054>

Appendix



Figure 1. Various axes produced through the Stone Age (Ref 1)



Figure 2. Axe heads from the Bronze Age including (left) palstave axe head and (right) socketed axe head (Ref 3)



Figure 4. Depiction of Sagaris axe held by a Scythian warrior on an Attic red-figure neck amphora (Ref 10)



Figure 5. Bearded axe head from around AD 1000 (Ref 16)



Figure 6. Dane axe head from around the second half of the 10th century (Ref 12)



Figure 7. Partial depiction of Bayeux Tapestry showing the use of battle-axes in the Battle of Hastings in 1066 (Ref 13)



Figure 8. Full depiction of the Battle of Bannockburn in the Holkham Bible Picture Book where the circled area includes the referenced axe. (Ref 15)



Figure 9. Horseman's axe from around 1475 that features holes for wrist straps and a belt loop (Ref 16)



Figure 10. Various axes with langets; (left) ornamental axe of Cardinal Ippolito de' Medici (Spain, 1511-1535) with steel langets (Ref 18) and (right) German horseman's axe (1490-1535) with brass langets covering the entirety of the wooden shaft (Ref 19)



Figure 11. Axes without langets (left) English horseman's axe (1600-1650) made of iron with wooden grip and iron guard (Ref 20) and (right) German horseman's axe (16th century) with a wrist strap but without langets or top spike instead using a more traditional method of fixturing (Ref 21)

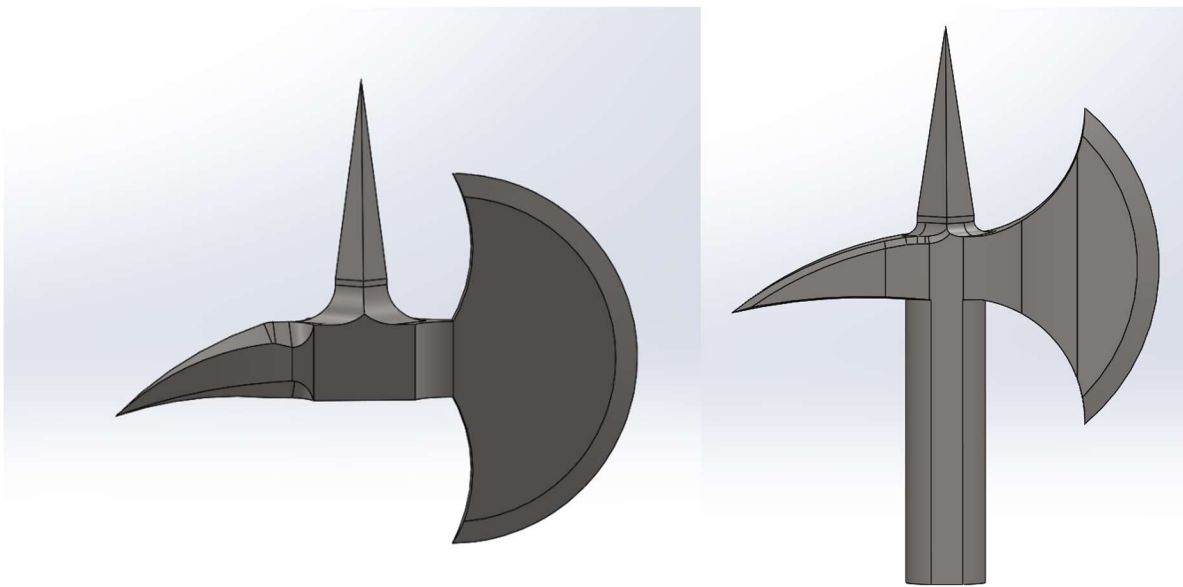
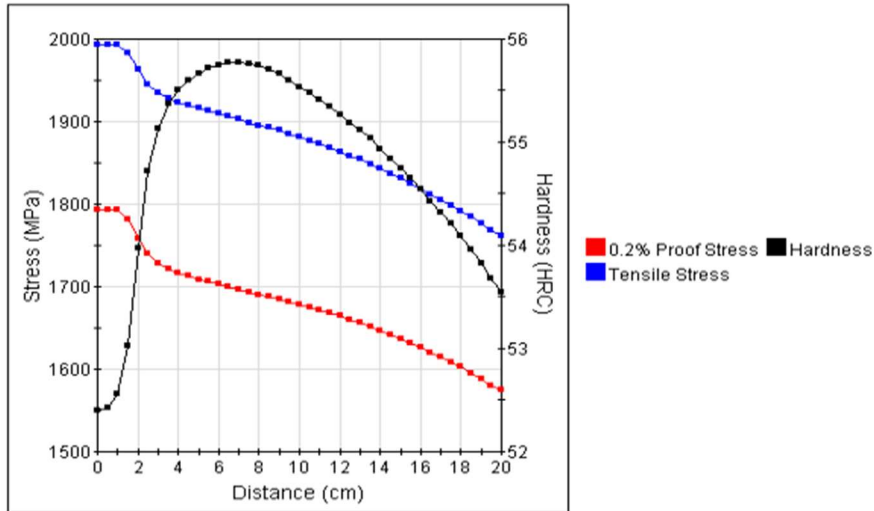


Figure 12. (left) Initial SolidWorks model of axe design and (right) Final SolidWorks model of axe design

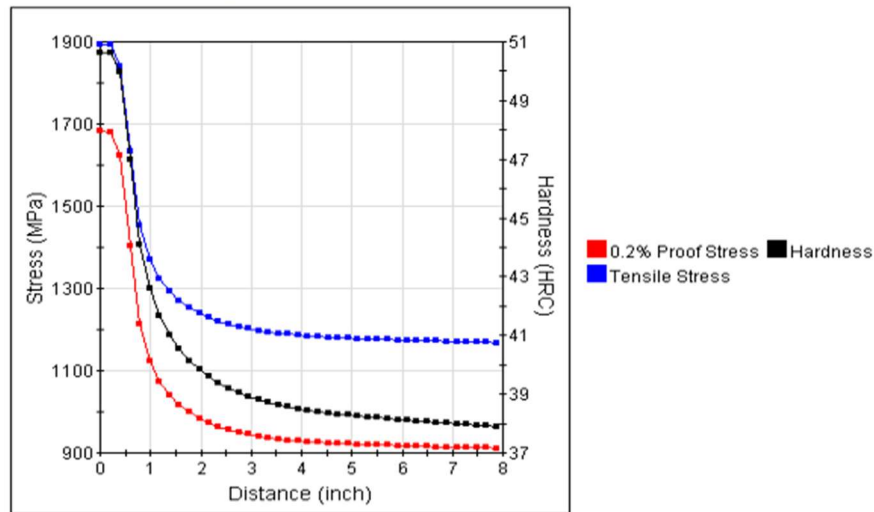
Jominy hardenability



Grain size : 30 microns
Austenitisation : 900.0 C

COMPOSITION (wt%)
Fe: 95.37
Cr: 1.7
Mn: 0.7
Mo: 0.35
Si: 1.6
C: 0.28

Jominy hardenability



Grain size : 30 microns
Austenitisation : 900.0 C

COMPOSITION (wt%)
Fe: 95.5
Cr: 0.8
Mn: 0.95
Mo: 0.45
Ni: 1.65
Si: 0.4
C: 0.25

Figure 13. JMatPro-v151 Jominy hardenability simulations of (top) CS1E0703 and (bottom) CS-28A

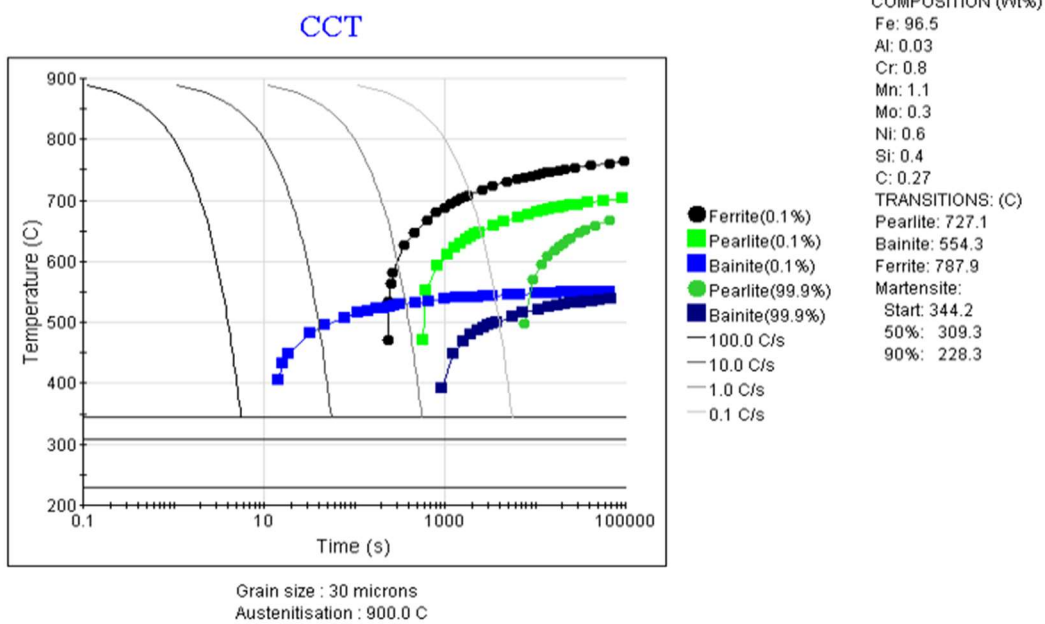
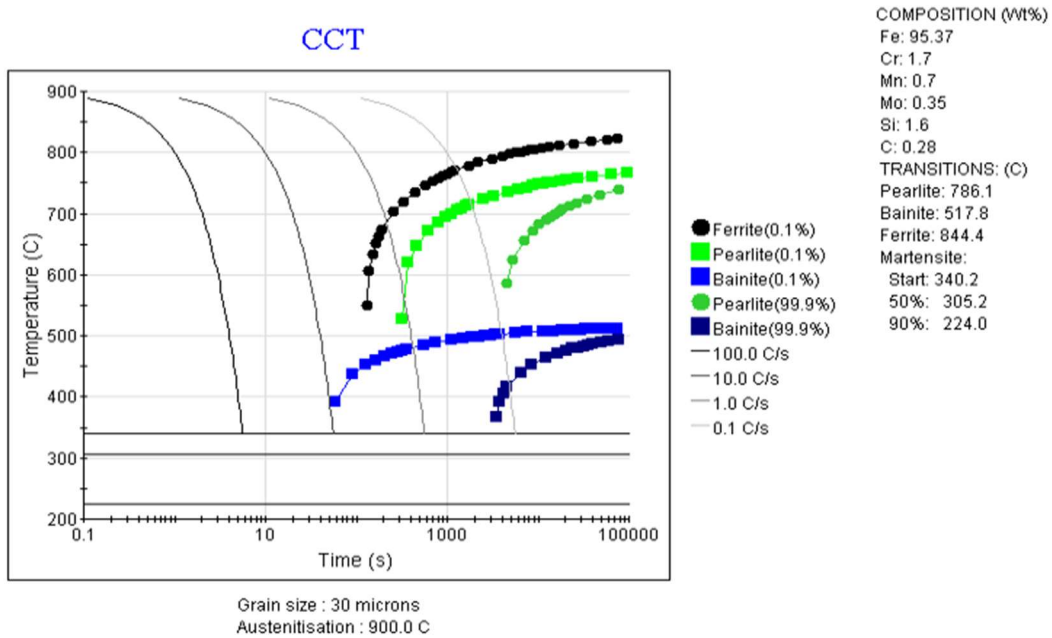


Figure 14. JMatPro-v151 CCT diagram simulations of (top) CS1E0703 and (bottom) CS-28A



Figure 15. Mold boxes built for sand casting

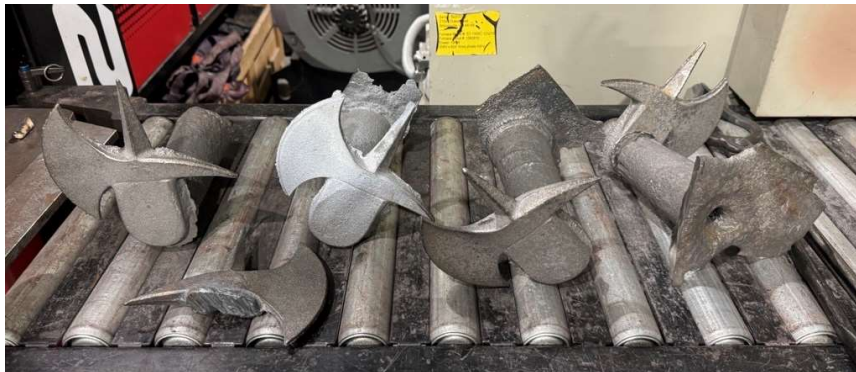


Figure 16. Casted axes with riser and sprue from Southern Cast Products



Figure 17. Drilled eye hole in bottom of axe



Figure 18. White ash block prior to sanding



Figure 19. Wood handle finished shape



Figure 20. Hot rolled ingot prior to cold rolling



Figure 21. Cold rolling process



Figure 22. Cold rolled steel prior to cutting



Figure 23. Water jetting langets and belt loop



Figure 24. Cut langets and belt loops



Figure 25. Forged belt loop final shape



Figure 26. Final langets and belt loop

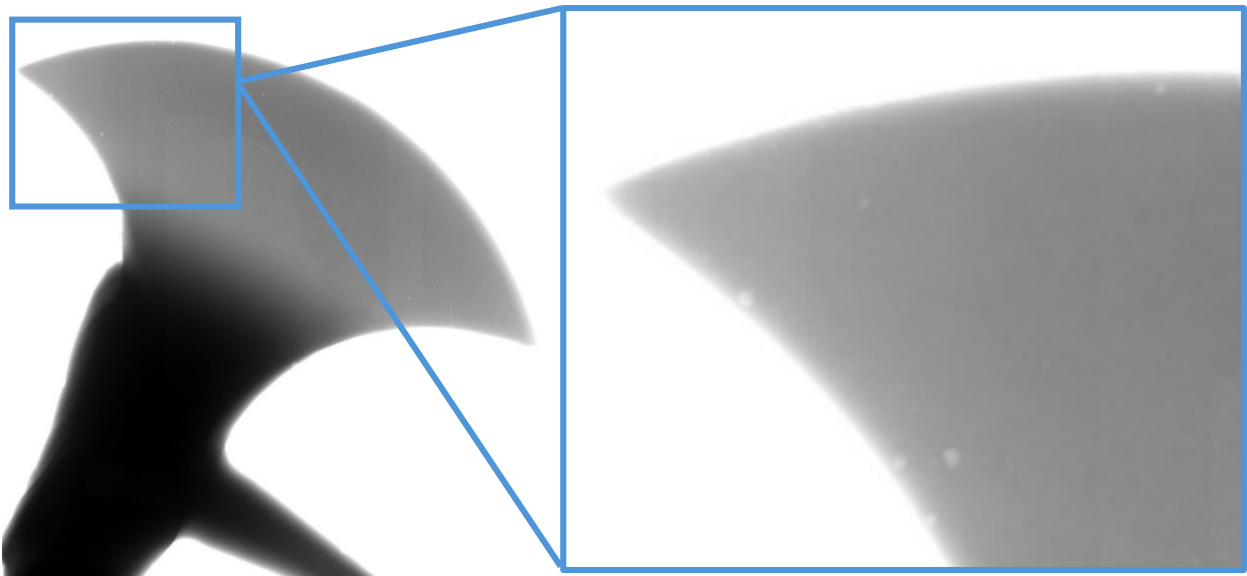


Figure 27. X-Ray CT scan of axe blade

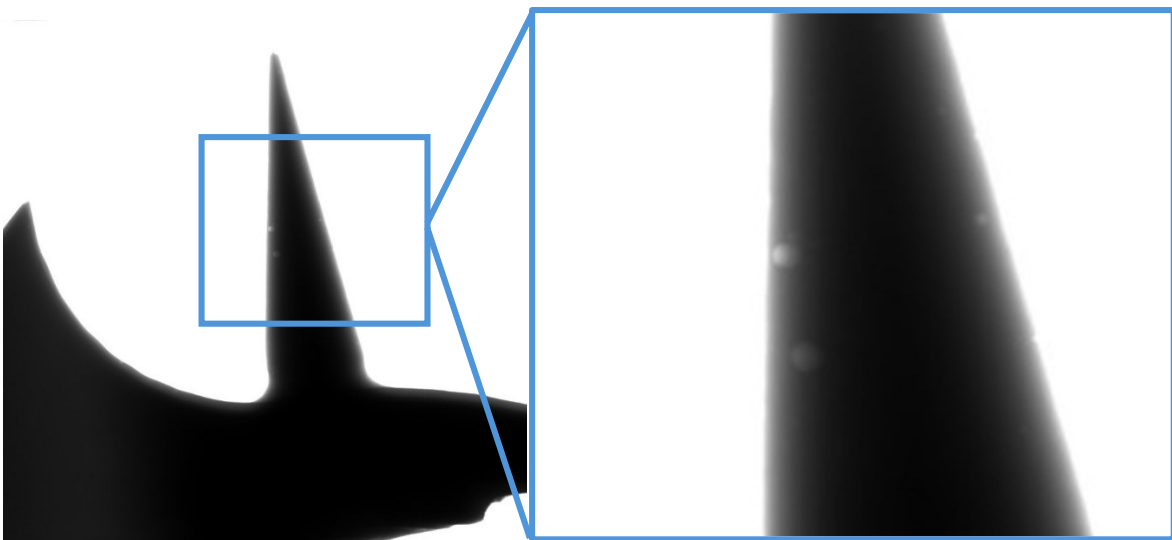


Figure 28. X-Ray CT scan of spike

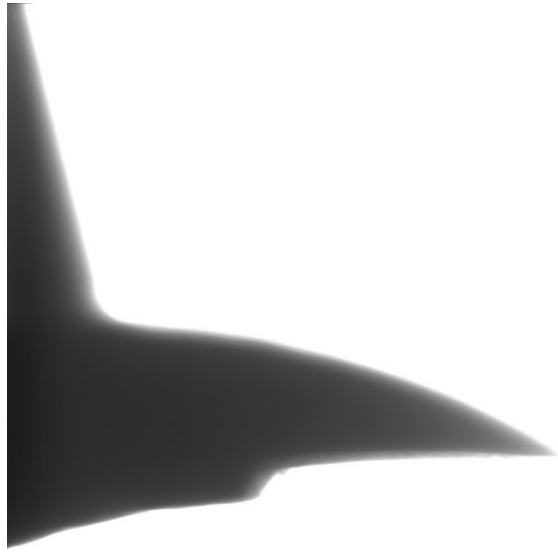


Figure 29. X-Ray CT scan of pick

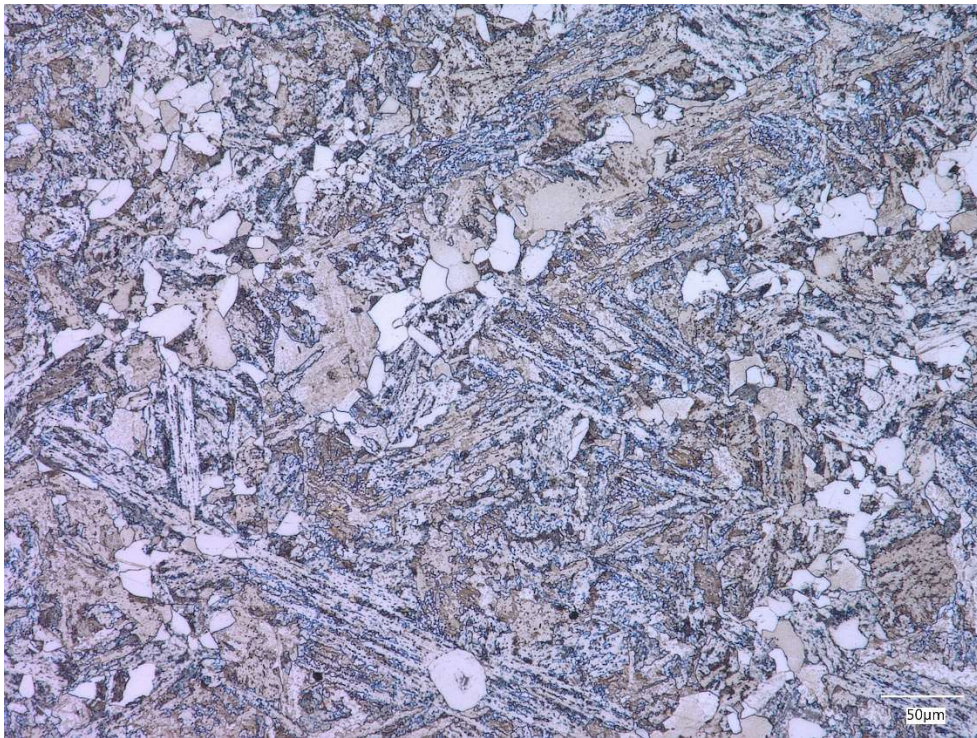


Figure 30. Post-annealing microstructure with 2% nital and 10% SMB

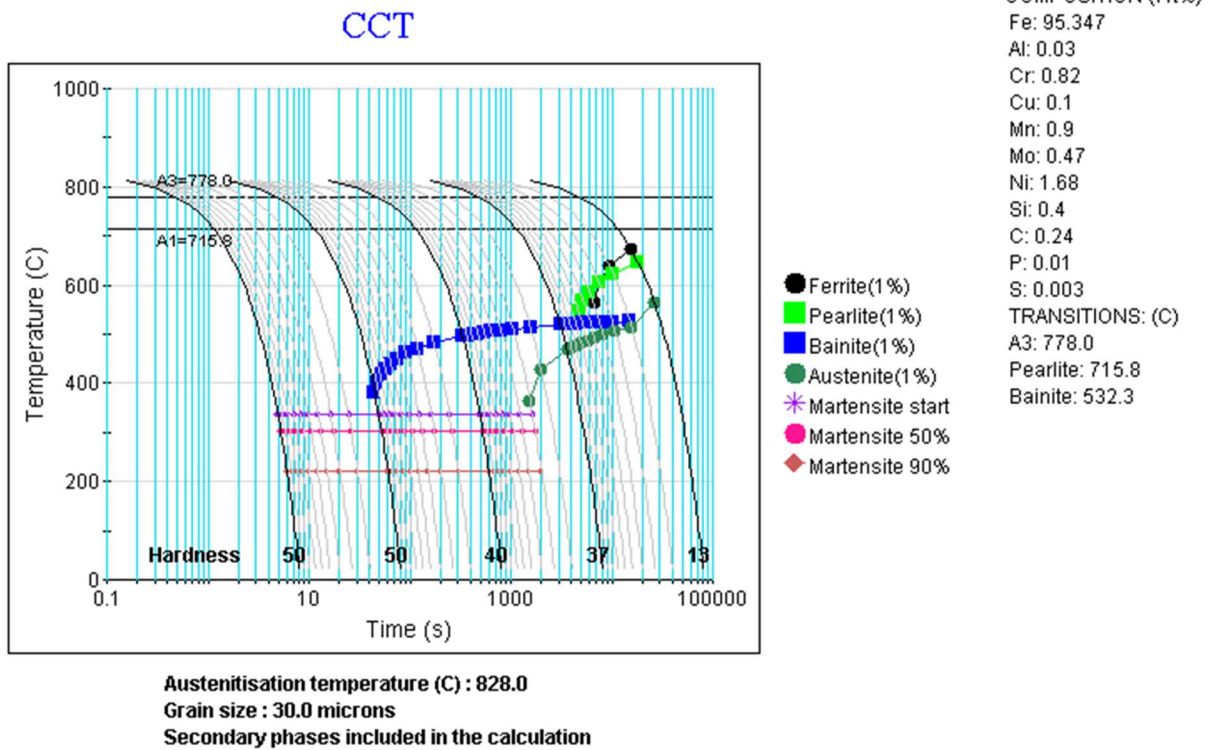


Figure 31. JMatPro-v151 final chemistry CCT diagram

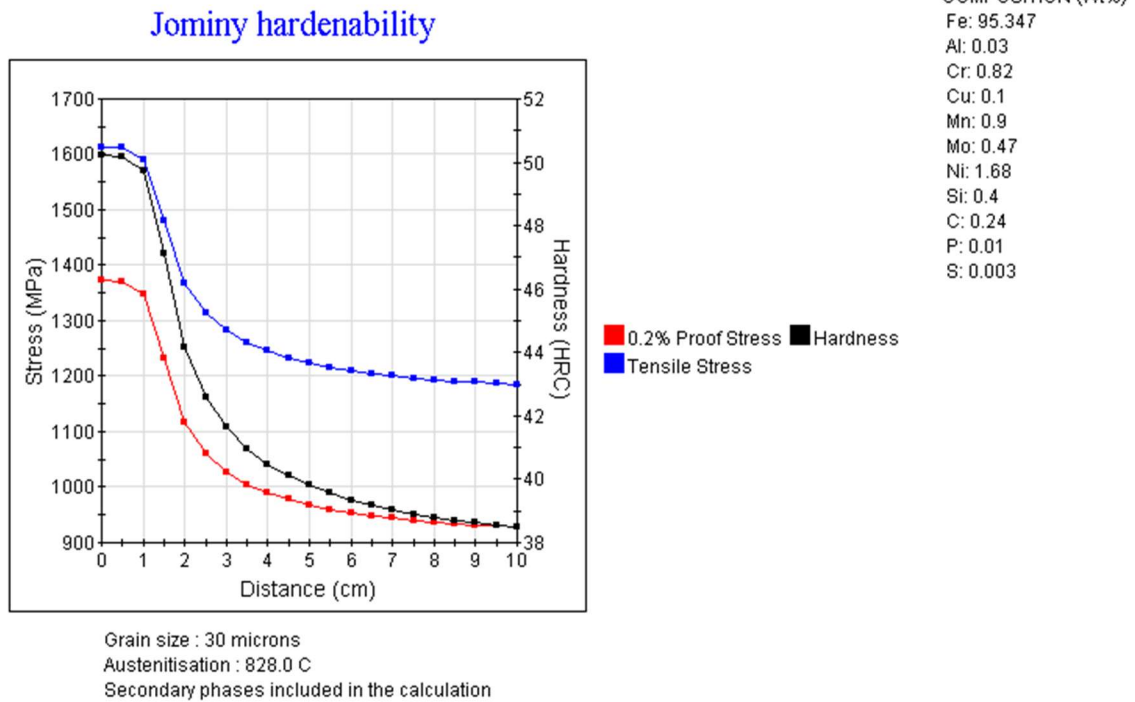


Figure 32. JMatPro-v151 Jominy hardenability simulations for final axe chemistry

Tempering

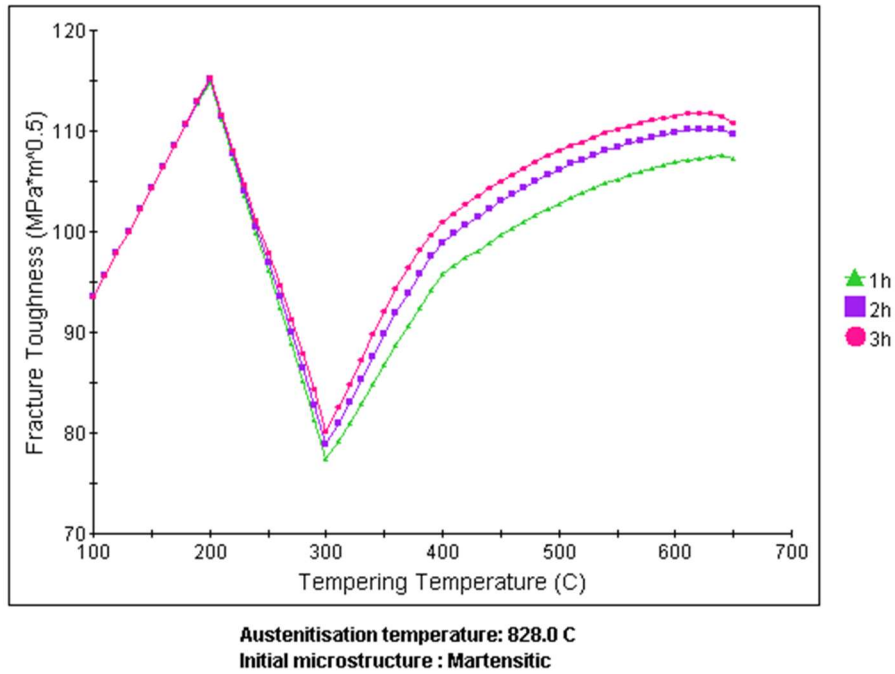


Figure 33. JMatPro-v151 simulation of fracture toughness vs. tempering temperature

Tempering

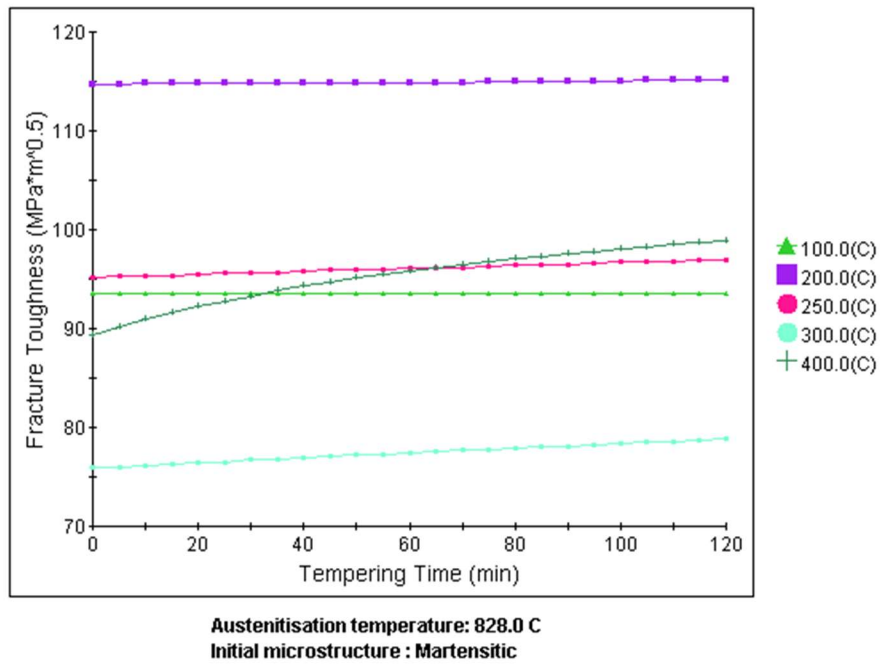
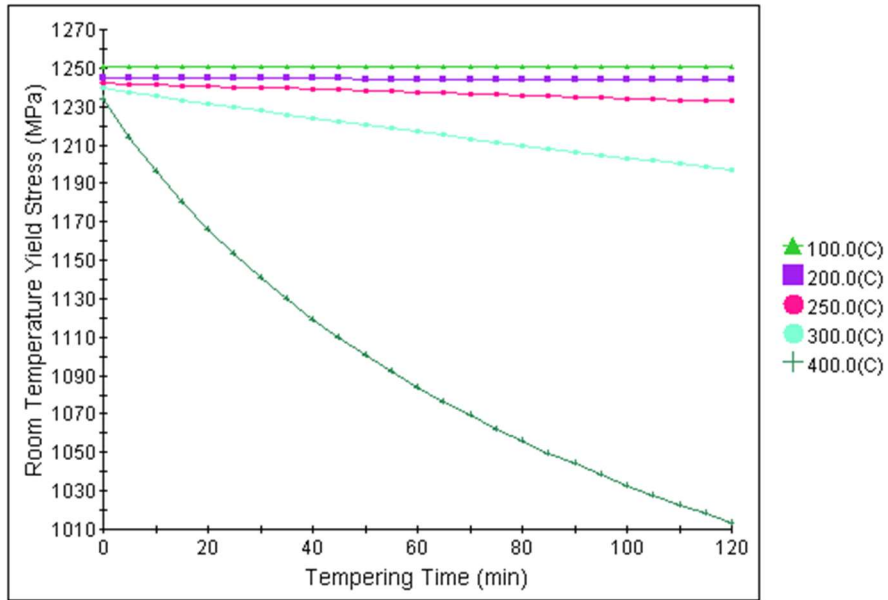


Figure 34. JMatPro-v151 simulation of fracture toughness vs. tempering time

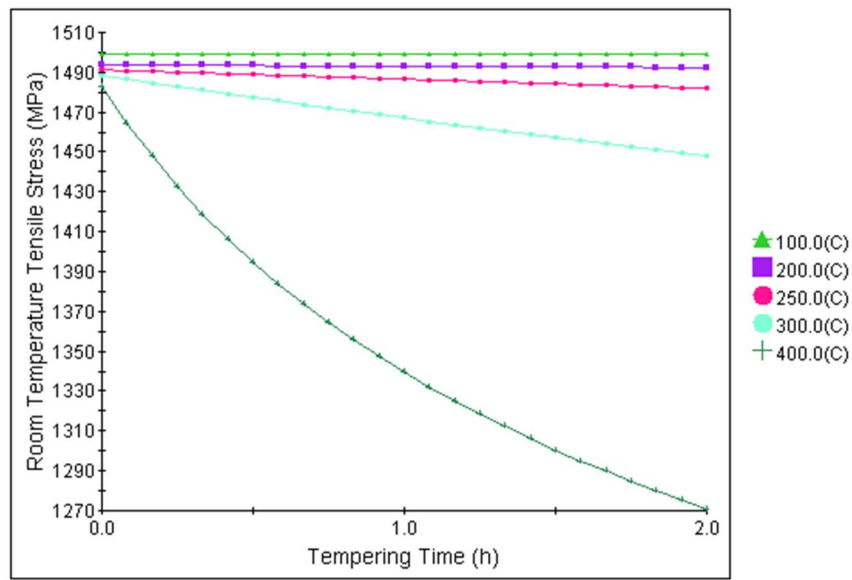
Tempering



Austenitisation temperature: 828.0 C
Initial microstructure : Martensitic

Figure 35. JMatPro-v151 simulation of yield stress vs. tempering time

Tempering



Austenitisation temperature: 828.0 C
Initial microstructure : Martensitic

Figure 36. JMatPro-v151 simulation of ultimate tensile stress vs tempering time

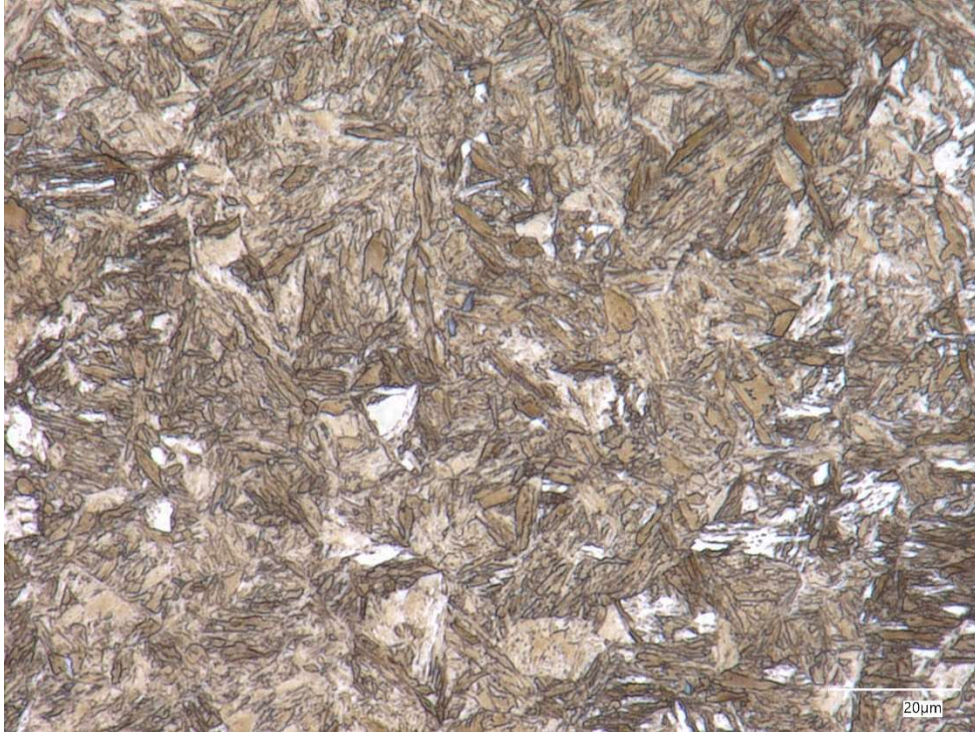


Figure 37. Quenched Microstructure with 2% nital and 10% SMB

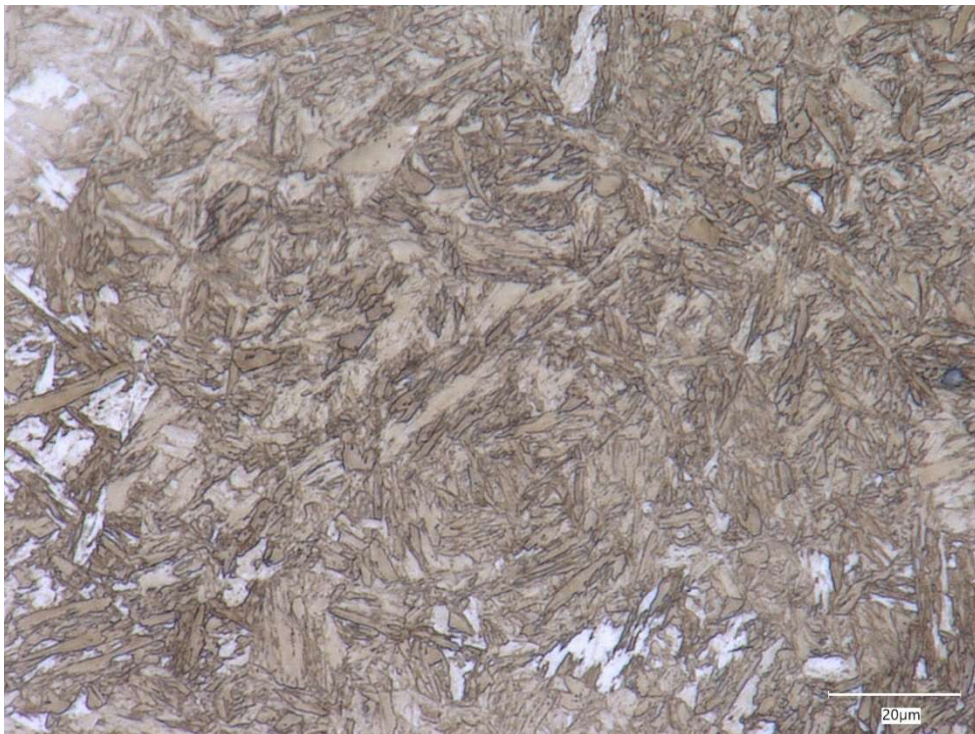


Figure 38. Quenched and tempered microstructure with 2% nital and 10% SMB

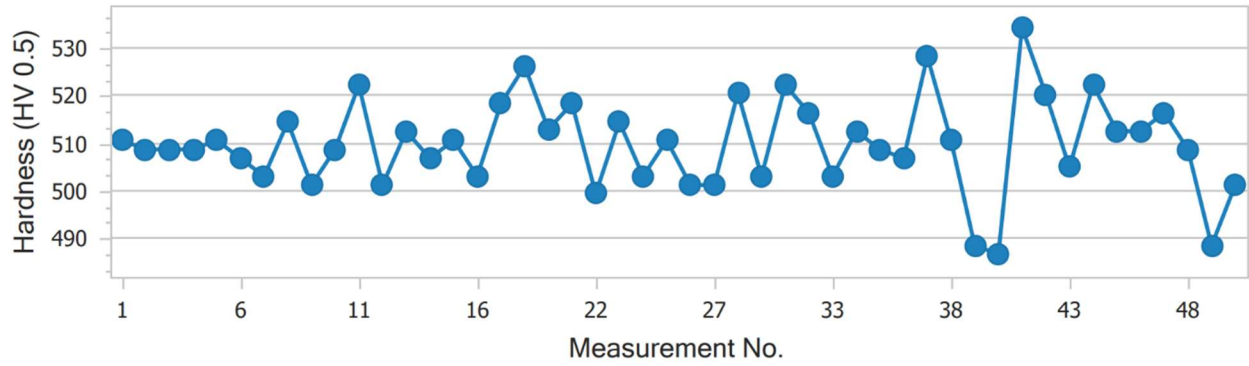


Figure 39. Results from Vickers Hardness test for quenched sample

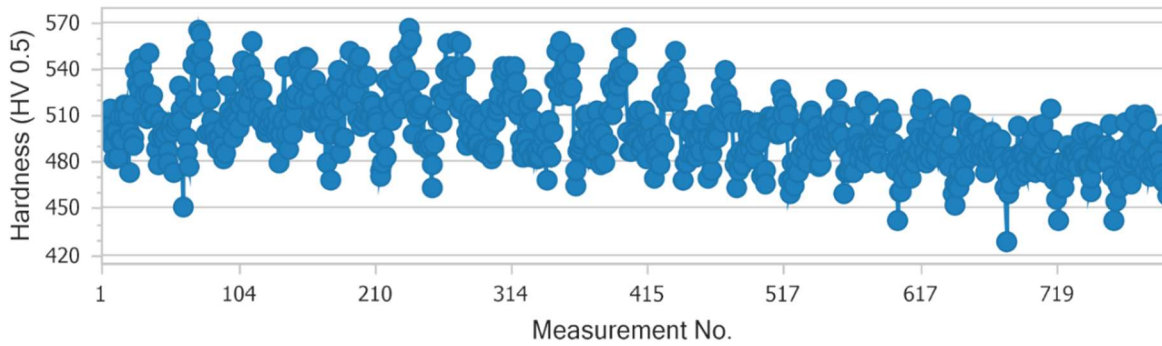


Figure 40. Results from Vickers Hardness test for quenched and tempered sample

Flow-Stress

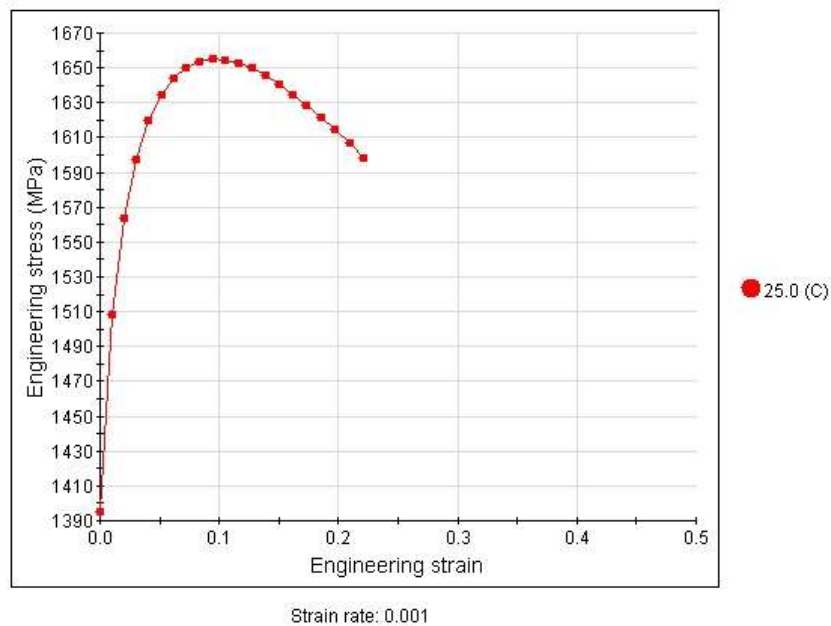


Figure 41: JMatPro-v151 simulation of tempered flow stress

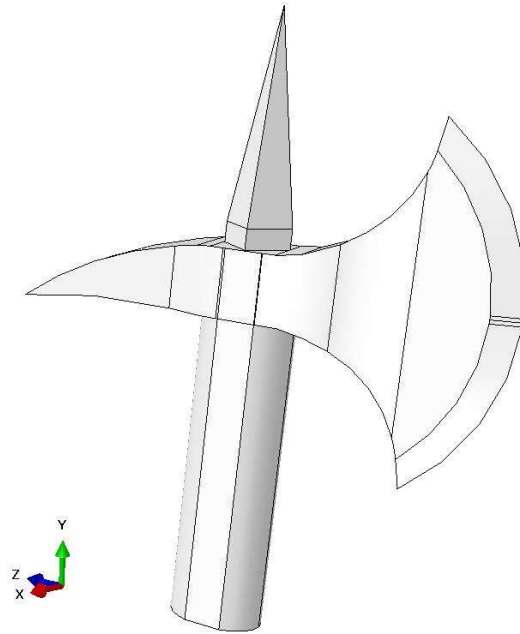


Figure 42. 3DS Simulia Abaqus FEA model of final axe

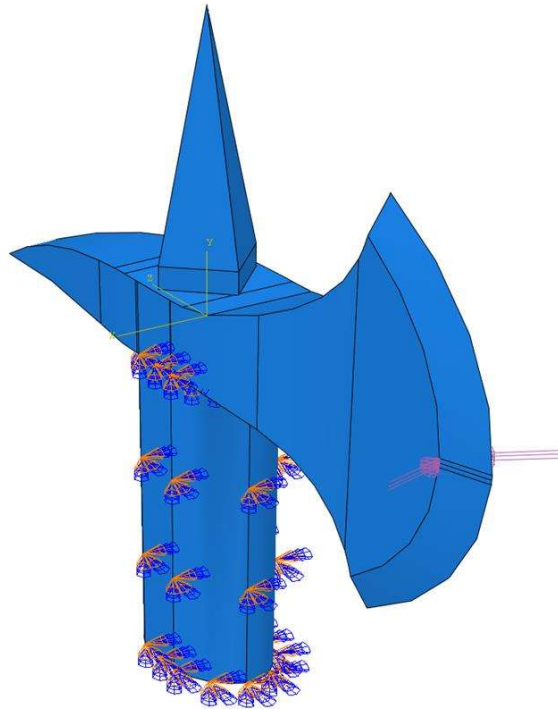


Figure 43. 3DS Simulia Abaqus FEA loading conditions for impact near the middle of the axe blade

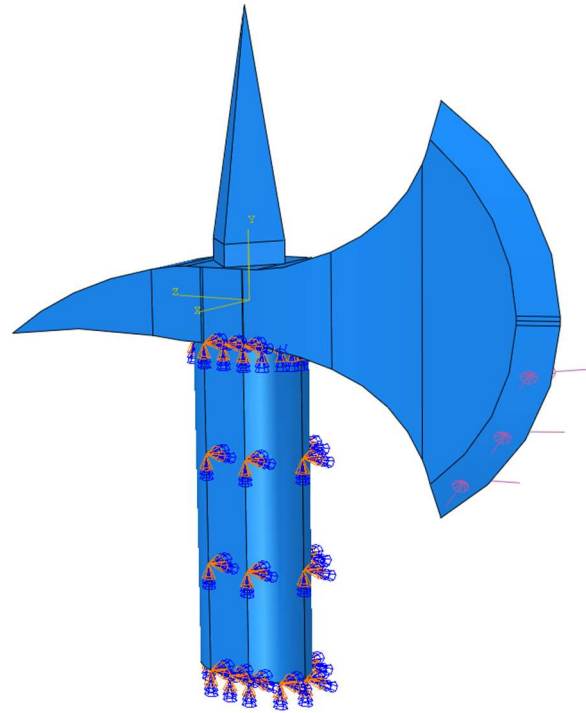


Figure 44. 3DS Simulia Abaqus FEA loading conditions for impact near the bottom of the axe blade

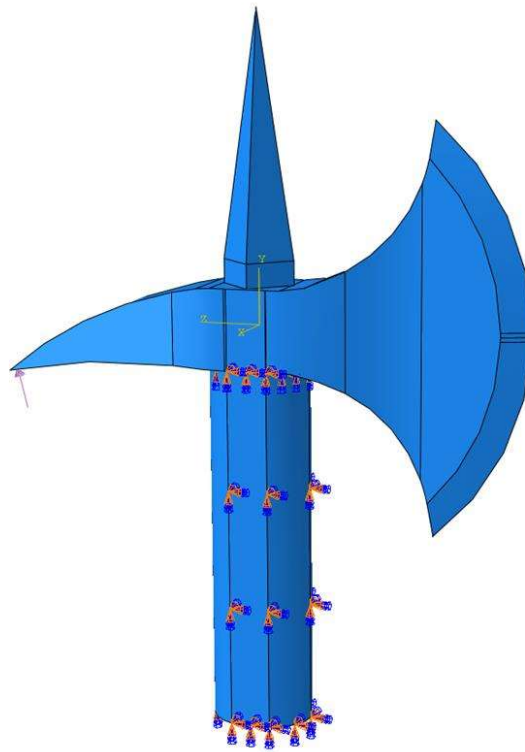


Figure 45. 3DS Simulia Abaqus FEA loading conditions for the pick

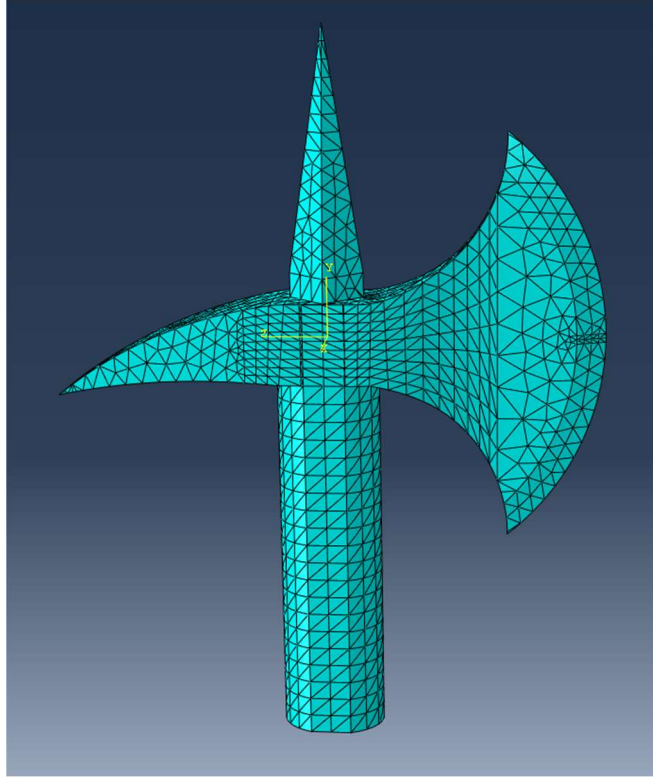


Figure 46. 3DS Simulia Abaqus FEA mesh for axe

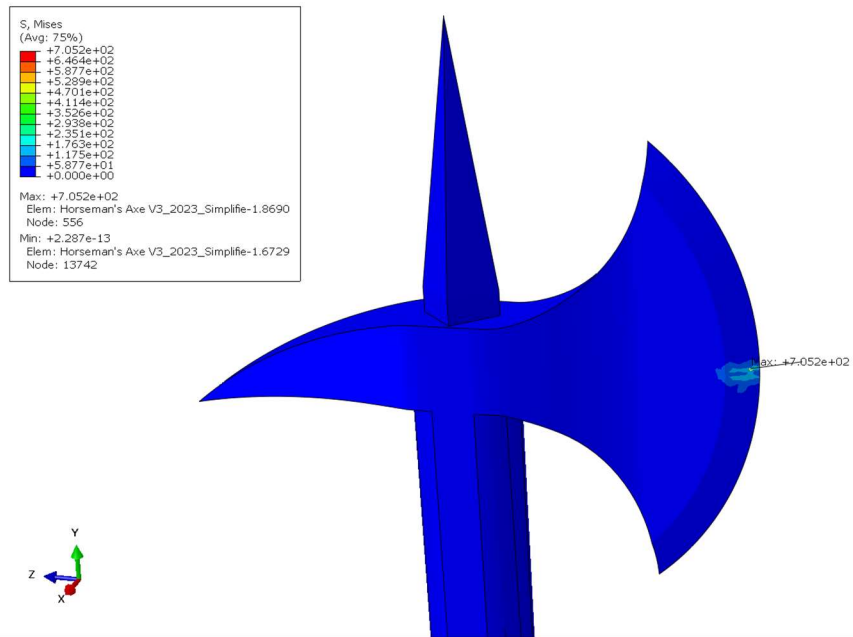


Figure 47. 3DS Simulia Abaqus FEA von Mises stress contour of center of the axe blade impacting plate metal

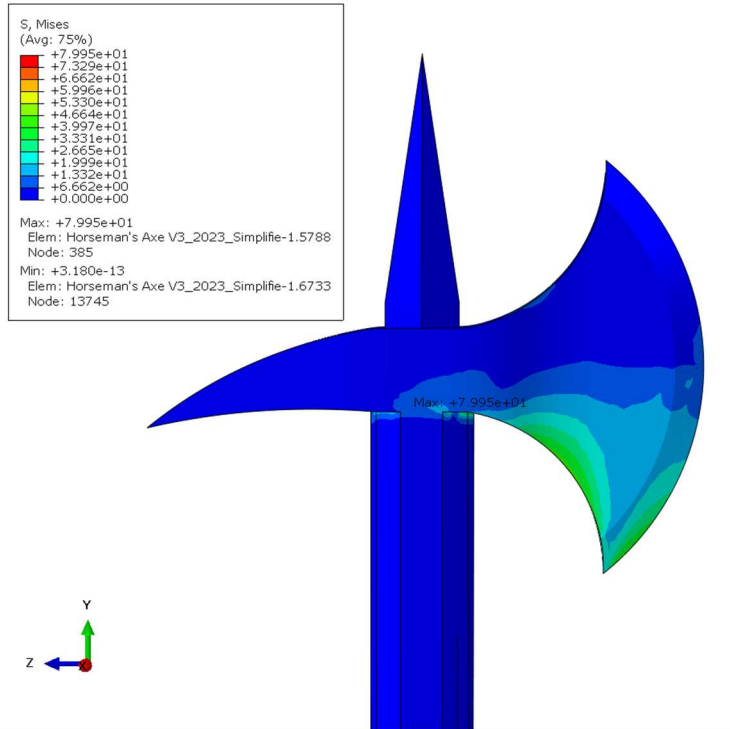


Figure 48. 3DS Simulia Abaqus FEA von Mises stress contour of lower edge of the axe blade impacting plate metal

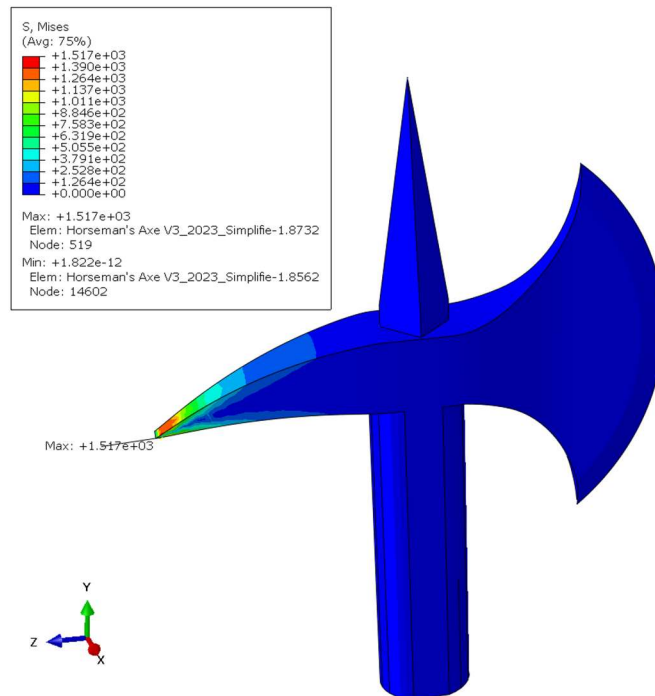


Figure 49. 3DS Simulia Abaqus FEA von Mises stress contour of pick of the axe impacting plate metal



Figure 50. Completed Axe

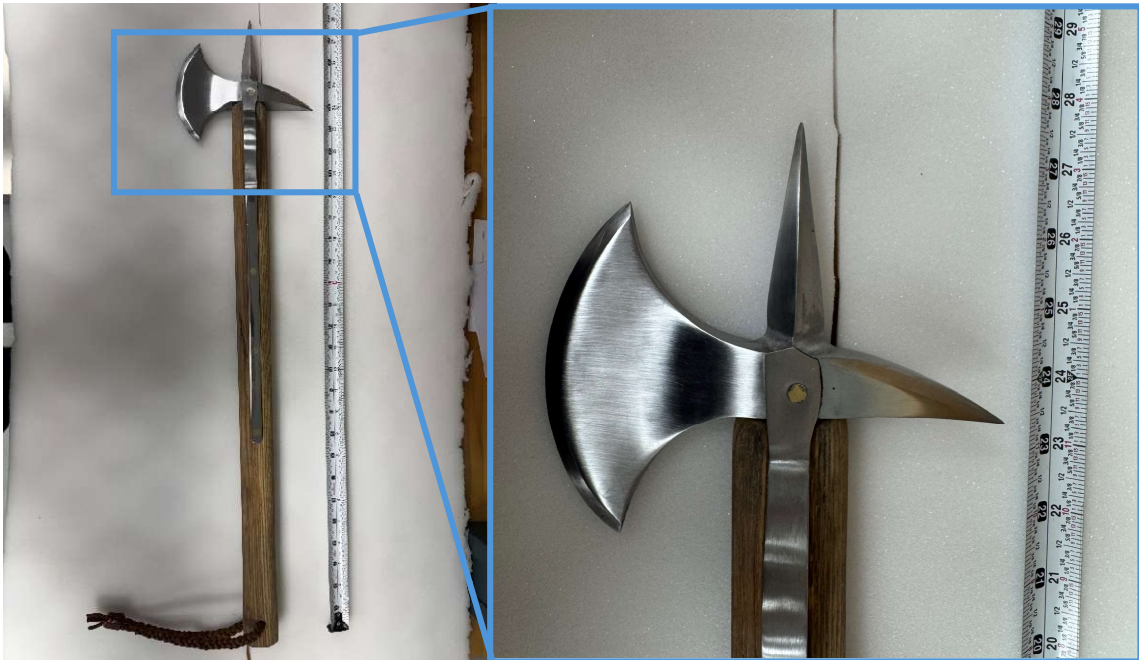


Figure 51. Length of final axe



Figure 52. Weight of final axe

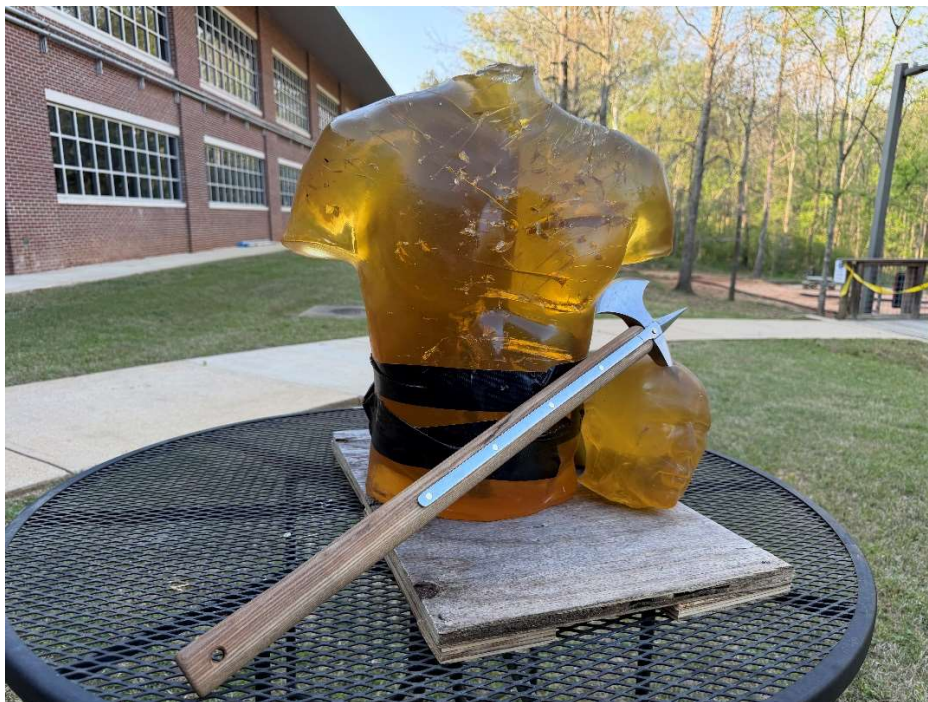


Figure 53. Testing of axe on ballistic gel dummy

Table 1. Horseman's Axe Dimensions

Axe	Length	Weight
Axe of Cardinal of Ippolito... (Ref 18)	30.75"	2.5 lbs.
German axe with brass languets (Ref 19)	27.875"	N/A
English axe with metal shaft (Ref 20)	29.5"	2.15 lbs.
German axe without languets (Ref 21)	22.375"	0.75 lbs. (head)

Table 2. Compositions for steel alloys (wt.%)

Alloy	Fe	C	Mn	Si	Cr	Ni	Mo	S	P	Al	Cu
CS-28A (Axe)	95.347	0.24	0.90	0.40	0.82	1.68	0.47	0.003	0.01	0.03	0.10
CS-28A	95.5	0.25	0.95	0.4	0.8	1.65	0.45	-	-	-	-
CS1E0703	95.37	0.28	0.7	1.6	1.7	-	0.35	-	-	-	-

Table 3. Data from Southern Cast Products

Ultimate Tensile Strength	163.3 KSI (1126 MPa)	Yield Stress	149.1 KSI (1028 MPa)
Elongation	16.1 %	Reduction of Area	41.7%
Lower BHN	302 (32 HRC)	Upper BHN	341 (37 HRC)
Charpy Value 1	17 ft lbs	Charpy Value 2	21 ft lbs
Charpy Value 3	22 ft lbs	Charpy Temperature	-40 °C

Table 4. 3DS Simulia Abaqus FEA set up for simulations

Material Assumptions	Elastic (Young's Modulus = 200 GPa; Poisson's Ratio = 0.3), Plastic (True Stress and True Strain calculated from flow curve)
Section	Solid, Homogenous
Step	Static, General
Boundary Conditions	Handle encastred
Loading Conditions	Force (12520 N) applied to various areas: Middle blade impact (247 MPa), Lower edge blade impact (10 MPa), pick impact (404 MPa)
Mesh Type	Tetrahedral
Number of Elements	8979

Equation 1. True stress calculation for plastic model in FEA simulation

$$\sigma_{true} = \sigma_{eng}(1 + \epsilon_{eng})$$

Equation 2. True strain calculation for plastic model in FEA simulation

$$\epsilon_{true} = \ln(1 + \epsilon_{eng})$$

Equation 3. Free-fall velocity derived from energy equations in potential energy and kinetic energy used for FEA calculations

$$v = \sqrt{2gh}$$

Where m is the mass of the axe in kg, g is the gravity of the Earth at 9.81 m/s², h is the height of the horse at 2 m, and v is the velocity in m/s.

Equation 4. Acceleration equation used for FEA calculations

$$a = \frac{v}{t}$$

Where a is the acceleration in m/s², v is velocity in m/s and t is the impact duration time in s

Equation 5. Force equation used for FEA calculations

$$F = ma$$

Where F is the force that is directed back to the axe, m is the mass of the axe in kg, and a is the found acceleration in m/s²